Chapter 5
Thresholds and Complex Dynamics of Interdependent Cascading Infrastructure Systems

B. A. Carreras, D. E. Newman, I. Dobson, V. E. Lynch and Paul Gradney

Abstract Critical infrastructures have a number of the characteristic properties of complex systems. Among these are infrequent large failures through cascading events. These events, though infrequent, often obey a power law distribution in their probability versus size which suggests that conventional risk analysis does not apply to these systems. Real infrastructure systems typically have an additional layer of complexity, namely the heterogeneous coupling to other infrastructure systems that can allow a failure in one system to propagate to the other system. Here, we model the infrastructure systems through a network with complex system dynamics. We use both mean field theory to get analytic results and a numerical complex systems model, Demon, for computational results. An isolated system has bifurcated fixed points and a cascading threshold which is the same as the bifurcation point. When systems are coupled, this is no longer true and the cascading threshold is different from the bifurcation point of the fixed point solutions. This change in the cascading threshold caused by the interdependence of the system can have an impact on the "safe operation" of interdependent infrastructure systems by changing the critical point and even the power law exponent.

B. A. Carreras
BACV Solutions, Inc., Oak Ridge, TN 37830, USA

D. E. Newman (✉) · P. Gradney
Physics Department, University of Alaska, Fairbanks, AK 99775, USA
e-mail: denewman@alaska.edu

I. Dobson
ECE Department, Iowa State University, Ames, IA 50011, USA

V. E. Lynch
Oak Ridge National Laboratory, Oak Ridge, TN 37831, USA

G. D'Agostino and A. Scala (eds.), *Networks of Networks: The Last Frontier of Complexity*, Understanding Complex Systems, DOI: 10.1007/978-3-319-03518-5_5,
© Springer International Publishing Switzerland 2014

5.1 Introduction

Many critical infrastructure systems exhibit the type of behavior that has come to be associated with "Complex System" dynamics. These systems range from electric power transmission and distribution systems, through communication networks, commodity transportation infrastructure and arguably all the way to the economic markets themselves. There has been extensive work in the modeling of some of these different systems. However, because of the intrinsic complexities involved, modeling of the interaction between these systems has been limited [1–3]. At the same time, one cannot simply take the logical view that the larger coupled system is just a new larger complex system because of the heterogeneity introduced through the coupling of the systems. While the individual systems may have a relatively homogeneous structure, the coupling between the systems is often both in terms of spatial uniformity and in terms of coupling strength, fundamentally different. Understanding the effect of this coupling on the system dynamics is necessary if we are to accurately develop risk models for the different infrastructure systems individually or collectively.

We have already investigated [4, 5] some of the effects of the coupling between systems by using a dynamical model of coupled complex systems, the Demon model. This model is an extension of the Complex System Models used to study forest fires [6, 7]. Here, we will focus on some particular aspects of this model, for which the coupling introduces some fundamental changes on the properties of the system.

This type of model is characterized by the existence of a bifurcated equilibrium. Here one equilibrium solution is such that all components of the system are working. The second type of equilibrium has a fraction of the components failed. As the load on the system increases (or the probability of failure propagation) there is a transition from the first type of equilibrium to the second, at a critical loading [8, 9]. In a single system, this transition point is also the threshold for cascading events of all sizes, that is, transitioning between "normally distributed events" [10] and large-scale failures.

The coupling between the systems can modify the system's behavior and therefore importantly, conditions for safe operation. In this model we introduce a possibility of failure propagation from one system to another not only when a component fails but also when a component is out of working order. This has two different effects. One is a tendency to keep some components failed while still in normal operation. How many depends on the ratio between the strength of the coupling and the repair rate. As we see later in this chapter, the "critical loading" bifurcation point of the equilibrium is reduced by a function of this ratio.

The second effect of the coupling is it allows propagation of failures from one system to the other during a cascading event. Therefore the cascading threshold is also lowered by an amount proportional to this coupling. Since the parameter controlling this effect is not the same as the one controlling the equilibrium bifurcation, the equilibrium bifurcation point and the cascading threshold are now different.

Because of these changes, the often used metrics [11–13] for determining the threshold for large scale cascading events in the system will be re-examined and we will study the effect of the coupling of the systems on these measures.

The rest of the chapter will be organized as follows: Sect. 5.2 gives a description of the coupled infrastructure model, Demon, and a summary of some of the results from that model. Section 5.3 introduces a mean field version of the model and uses it to study the possible steady state solutions. The dynamics from the perspective of the mean field theory is described in Sect. 5.4 and in Sect. 5.5 the results of this analysis is compared with the numerical solutions of the mean field model. Then in Sect. 5.6, the results of the mean field theory are compared with the results of the dynamical model Demon. Finally, in Sect. 5.7, a discussion of the implications of these results and conclusions are presented.

5.2 The Demon Model

The infrastructure model discussed here, the Demon model, is based on the forest fire model of Bak et al. [7] with modifications by Drossel and Schwabl [6].

For a single system, the model is defined on a user defined 2-D network. An example of such network is shown in Fig. 5.1. Nodes represent components of the infrastructure system and lines represent the coupling between components. These components can be operating, failed or failing. The rules of the model for each time step are:

(1) A failed component is repaired with probability P_{r}.
(2) A failing component becomes a failed one.
(3) An operating component fails with a probability P_{n} if at least one of the nearest components is failing.
(4) There is a probability P_{f} that any operating component fails.

The Demon model [4] considers a coupled system by taking two of these 2-D networks and adding another rule:

(5) A component in System 1 can fail with a coupling parameter c, if the associated component in System 2 is failed or failing. The same applies for a component in system 2.

The ordering of the four parameters in the model is very important as discussed in [6]. Here, for the particular infrastructure problem, the different probabilities can be directly related to the characteristic times of repair, failure, and propagation of failure. It is worth noting that the propagation of failure parameter, P_{n}, is closely related to the loading of the system in a real infrastructure or a more realistic infrastructure model such as those described in [8, 14, 15]. This means that in the real infrastructures and more realistic models, there is an additional feedback that moves the system to near its critical point. We will use data from the power transmission system as guidance for those values. A more difficult parameter to characterize is the parameter that measures the coupling between the systems. The ability to explore the couplings between systems is an important flexibility in Demon as real world systems can have a wide variety of couplings that can impact their dynamics. For example they can be coupled mono-directionally (often,

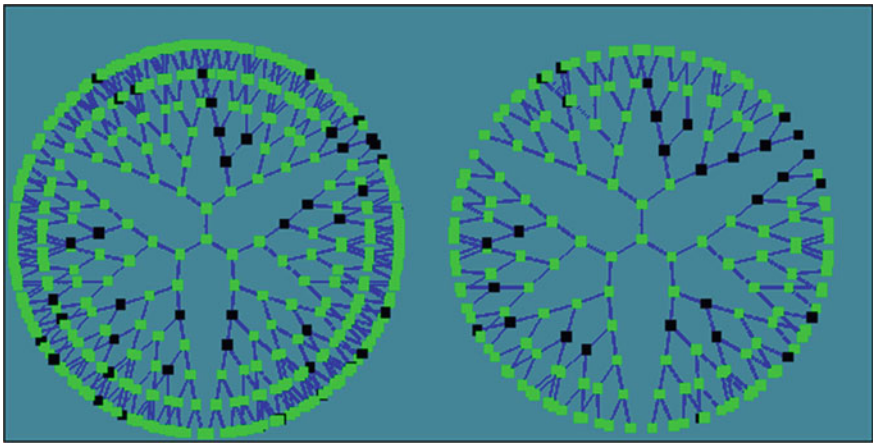

Fig. 5.1 A pair of tree networks used for the modeling as an example

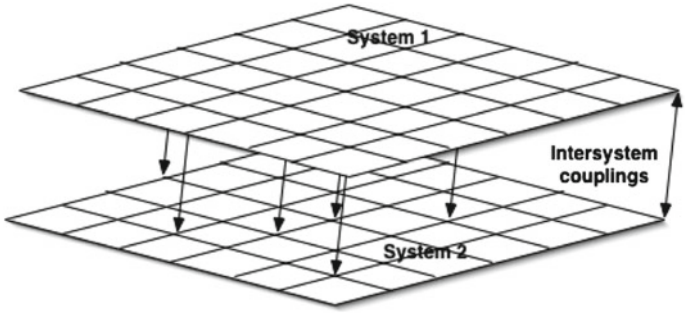

Fig. 5.2 A cartoon of the coupled networks, note that the number of nodes coupled between systems can be varied as can the strength, sign and directionality of the coupling

though not always, for pipeline-communications systems) or bi-directionally (most other systems, i.e. power transmission-communications systems), fully symmetric or asymmetric coupling strengths (failure in power transmission system has stronger impact on communications system then the other way around), homogeneously or heterogeneously (general spatial or course grained in one direction), negative reinforcement (power transmission-communications) or positive (perhaps infrastructure systems—decision making "system"). A cartoon of this type of coupled system is shown in Fig. 5.2. For most of the work described here we will use the simplest types of couplings, namely symmetric, homogeneous and with negative reinforcement.

Using these rules, numerical calculations can be carried out, the dynamics and critical behavior investigated and impacts of system structure explored.

This model is an extension of a previous model [4] based on square grid networks to consider arbitrary network structures. Therefore, the basic coupling was from each node to four neighbors. The model in [4] was in turn a simple extension of the

Table 5.1 Network properties

Type	K	Number of nodes
Open 3-branch tree	2	3070
Closed 3-branch tree	3	3070
Open 5-branch tree	4	190
Square	3.96	10000
Hexagon	5.9	4681

Drossel model [6] for forest fires with the added rule number 5 that leads to nontrivial differences between those models. In the forest fire model, the propagation velocity of a disturbance is $P_{\mathrm{n}} f$ where P_{n} is the probability of a disturbance to propagate from a node to another node and f the number of available nodes to propagate to, from a given node. In this model f is an important parameter to understand the propagation of the disturbances and it is not well determined. If K is the averaged number of nodes coupled to a single node in a given network, a first guess for f is $f = K - 1$, because the disturbance is already coming from one of the nodes that the failing node is coupled. In the case of the square network it was found [6] that $f = 2.66$ is a better value than 3. Therefore, we vary K in order to understand what the possible values are for f. In Table 5.1 we have summarized some of the properties of the different networks that we have considered in this chapter.

We will briefly look first at some of the results from this model, then we will investigate the mean field theory for this model and finally in Sect. 5.6 we will discuss the comparison between the mean field theory and the Demon model results.

When the control parameter, P_{n}, exceeds a critical (percolation) value the coupled system exhibits characteristics of a critical complex system. This critical value for an uncoupled system is given approximately by $P_{\mathrm{n}} f = 1$, which is when the failures have a non-zero probability of propagating across the entire system. For the full-coupled system, the coupling between the two systems modifies this value. If the cross system coupling were the same as the coupling between nodes in each system, this would be the same as a larger system whose average node degree (effectively K) is increased by one. When the two systems being coupled are identical, but with a coupling strength different, typically much smaller, then P_{n}, the size distribution of failures obeys a power law which is close to -1 for all of the network structures examined. Below this critical value, the systems display an exponential distribution of failure size. An instructive exercise can be carried out by having the probability of random failures, P_{f}, non-zero in only one of the coupled systems. In this case it is found that if P_n is above the critical value and the coupling between the systems is also non-zero, the system in which there are no random failures also exhibits the characteristic power law size distribution (Fig. 5.3). This means that systems that look robust can actually be vulnerable when coupled making analysis of the entire coupled system critical. This cross system propagation is of course due to the coupling and can be seen in the synchronization of the failures in the two systems.

Using a measure developed by Gann et al. [16] for synchronization, which is basically an average normalized difference between events in the two systems, we

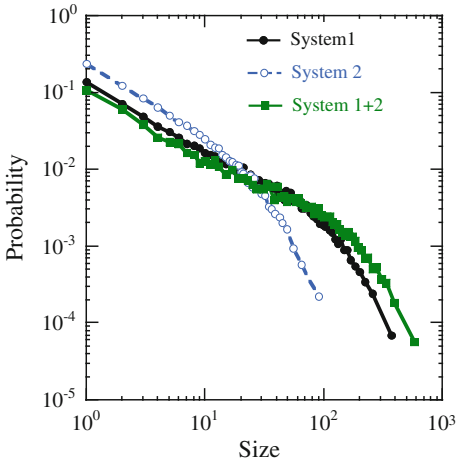

Fig. 5.3 The probability distribution functions of the failure sizes for a coupled system in which only system 1 has random failures but system 2 still has a power law PDF and the combined system has a heavier tail then an uncoupled system would

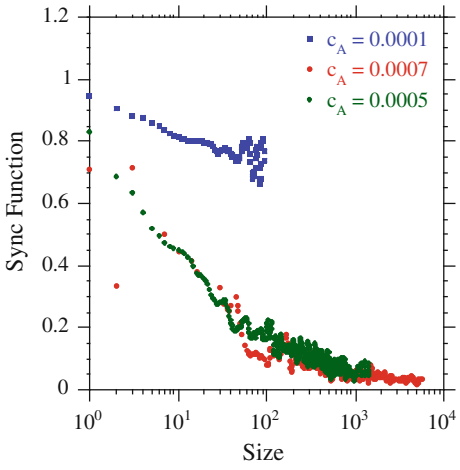

Fig. 5.4 The synchronization function as a function of size for a coupled system and three values of the coupling coefficient. Since 0 is fully synchronized and 1 is completely unsynchronized, it can be seen that the synchronization is stronger for larger failures and increases then saturates for larger values of coupling strength

investigate this effect. For this measure, a value of 1 means the difference is effectively 100 % or no synchronization, while a value of 0 means all events are the same in the two systems, or they are synchronized. For the Demon model it is found that large failures are more likely to be "synchronized" across the two dynamical systems, Fig. 5.4, as seen by the decrease in the synchronization function (which is an increase in the actual synchronization) as a function of size. This means that in the coupled systems there is a greater probability of large failures and lesser probability of smaller failures. This in turn causes the power law found in the probability of failure with size to be less steep, Fig. 5.5, with the coupling (i.e. the risk of larger failures is even higher in the coupled system). Above a certain value of the coupling, this effect saturates as the largest events are fully synchronized. The value of slope of the power

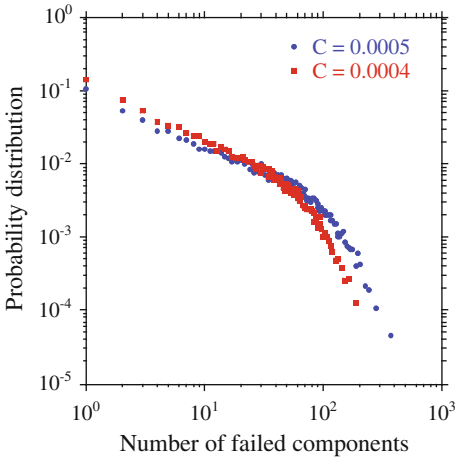

Fig. 5.5 PDF tail gets heavier as the coupling strength increases and then, as with the synchronization, saturates and stops changing

law for the coupled square grid with parameters given earlier approaches ~ -0.8 in contrast to ~ -1.0 for the uncoupled system.

The other major impact of the coupling on the system characteristics is the reduction of the critical point. As the coupling increases, the critical value of P_{n}, and by extension the loading, rapidly decreases (Fig. 5.6). This means that in an infrastructure system which by itself is nominally subcritical, the coupling, even weakly, to another infrastructure can make the entire system critical. This reduction will be further discussed in the next section on mean field theory of the coupled systems.

5.3 Mean Field Theory: Steady State

Let us consider first the mean field theory for two coupled systems. This is a generalization of the calculation as done in [6]. Let $O^{(i)}(t)$ be the number of operating components in system i at time t normalized to the total number of components $N^{(i)}$. In the same way, we can define the normalized number of failed components, $F^{(i)}(t)$, and the failing ones, $B^{(i)}(t)$. The mean field equations for this coupled system are:

$$B^{(1)}(t+1) = P_f^{(1)} O^{(1)}(t) + P_n^{(1)} f^{(1)} O^{(1)}(t) B^{(1)}(t) + \frac{c^{(1)}}{\mathcal{K}} g_2 O^{(1)}(t) \left(B^{(2)}(t) + F^{(2)}(t) \right) \tag{5.1}$$

$$F^{(1)}(t+1) = \left(1 - P_r^{(1)}\right) F^{(1)} + B^{(1)}(t) \tag{5.2}$$

$$O^{(1)}(t+1) = \left(1 - P_f^{(1)}\right) O^{(1)}(t) + P_r^{(1)} F^{(1)}(t) - P_n^{(1)} f^{(1)} O^{(1)}(t) B^{(1)}(t)$$

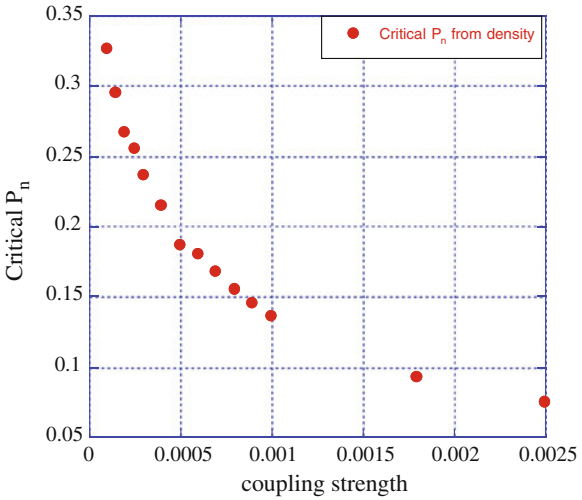

Fig. 5.6 The critical point decreases rapidly as the coupling strength increases. Even the maximum coupling strength is much less then the propagation coefficient within one system but the critical parameter has fallen by more than a factor of three

$$- \frac{c^{(1)}}{\mathcal{K}} g_2 O^{(1)}(t) \left(B^{(2)}(t) + F^{(2)}(t) \right) \tag{5.3}$$

$$B^{(2)}(t+1) = P_f^{(2)} O^{(2)}(t) + P_n^{(2)} f^{(2)} O^{(2)}(t) B^{(2)}(t) + \mathcal{K} c^{(2)} g_1 O^{(2)}(t) \left(B^{(1)}(t) + F^{(1)}(t) \right) \tag{5.4}$$

$$F^{(2)}(t+1) = \left(1 - P_r^{(2)}\right) F^{(2)}(t) + B^{(2)}(t) \tag{5.5}$$

$$O^{(2)}(t+1) = \left(1 - P_f^{(2)}\right) O^{(2)}(t) + P_r^{(2)} F^{(2)}(t) - P_n^{(2)} f^{(2)} O^{(1)}(t) B^{(2)}(t) - \mathcal{K} c^{(2)} g_1 O^{(2)}(t) \left(B^{(1)}(t) + F^{(1)}(t) \right). \tag{5.6}$$

Here $\mathcal{K} = N^{(1)}/N^{(2)}$, g_1 is the fraction of nodes in system 1 coupled to system two, and g_2 is the fraction of nodes in system 2 coupled to system 1. Of course, these equations are consistent with the conditions:

$$O^{(i)}(t) + B^{(i)}(t) + F^{(i)}(t) = 1 \tag{5.7}$$

In the limit with no failure triggers, $P_f^{(i)} = 0$, and for a steady state solution, the system of equations can be reduced to two coupled equations,

$$\left[1 - P_n^{(1)} f^{(1)} O^{(1)}\right]\left(1 - O^{(1)}\right) = \frac{a^{(1)}}{\mathcal{K}} g_2 \left(1 - O^{(2)}\right) O^{(1)} \tag{5.8}$$

$$\left[1 - P_n^{(2)} f^{(2)} O^{(2)}\right]\left(1 - O^{(2)}\right) = \mathcal{K} a^{(2)} g_1\left(1 - O^{(2)}\right) O^{(2)} \tag{5.9}$$

where

$$a^{(i)} = \frac{c^{(i)}\left(1 + P_r^{(i)}\right)}{P_r^{(i)}}. \tag{5.10}$$

It is important to note that the relevant parameter involves the ratio of the coupling between the systems to the repair rate. The reason for that is the particular form of rule (5) that assumes that a failure can be triggered by both failed and failing components in the other system. If only failing components had been considered, the relevant parameter would be the coupling. For real systems, a realistic rule should probably be in between these two.

If $a^{(\mathrm{i})} \neq 0$ and $\kappa = 1$, then $O^{(1)} = 1$ implies $O^{(2)} = 1$, that is, the systems are decoupled. Therefore, to have truly coupled systems, system 1 must be in a supercritical state. Such case with $a^{(\mathrm{i})} \neq 0$ is more complicated to solve.

First, we assume identical systems symmetrically coupled. That is, all parameters are the same for the two systems, $f^{(1)} = f^{(2)}$, $a^{(1)} = a^{(2)}$, $\kappa = 1$ and $P_{(n)}^{(1)} = P_{(n)}^{(2)}$. This leads to identical solutions for the two systems in steady state. Therefore, we have the following solutions:

$$O_{1eq}^{(i)} = 1, \quad F_{1eq}^{(i)} = 0, \quad B_{1eq}^{(i)} = 0 \tag{5.11}$$

and

$$O_{2eq}^{(i)} = \frac{1}{\hat{g}}, \quad F_{2eq}^{(i)} = \frac{\hat{g} - 1}{\hat{g}\,(1 + P_r)}, \quad B_{2eq}^{(i)} = \frac{\hat{g} - 1}{\hat{g}\,(1 + P_r)} P_r \tag{5.12}$$

The second solution is only valid for $\hat{g} > 1$. Here, $\hat{g}$ is the control parameter and is given by

$$\hat{g} = P_n f + \frac{c\left(1 + P_r\right)}{P_r} \tag{5.13}$$

In Eqs. (5.11) and (5.12) the subindex *eq* indicate that is an equilibrium solution.

The bifurcation point of the fixed point, $\hat{g} = 1$, has been decreased from the decoupled case, $P_n f = 1$, by a term proportional to c/P_r. Therefore, in general this reduction is considerably larger than the magnitude of the coupling itself.

We have tested the results from the mean field theory by comparing them with numerical results from some of the two-coupled identical systems networks listed in Table 5.1. The results for the averaged number of operating components are shown in Fig. 5.7. Results have been obtained for fixed $P_{\mathrm{r}} = 0.001, \mathrm{c} = 0.0005$, $P_{\mathrm{f}} = 0.00001$ (for system 1) and $P_{\mathrm{f}} = 0$ (system 2), and we have varied the propagation parameter P_{n}. The numerical results show very good agreement with the mean field theory results as K increases. For $K = 2$, the systems are practically one-dimensional and the mean field theory is not really applicable.

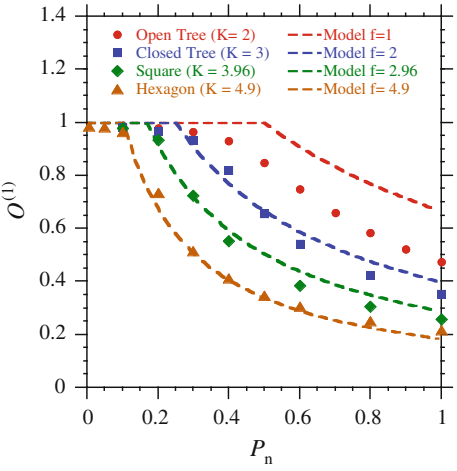

Fig. 5.7 The normalized operating components for various configurations

The density of operating components is practically the same in both systems. This is logical because they are identical systems the only symmetry breaking feature is the probability of spontaneous failures that is zero in the second system.

5.4 Mean Field Theory: Time Evolution

We will continue to assume the two systems are identical, in this way, we can simplify the system of Eqs. (5.1)–(5.6) to the following system:

$$B(t+1) = P_n f O(t) B(t) + c O(t)\big(B(t) + F(t)\big) \tag{5.14}$$

$$F(t+1) = \big(1 - P_r\big) F(t) + B(t) \tag{5.15}$$

$$O\,(t) + F\,(t) + B\,(t) = 1. \tag{5.16}$$

We have eliminated the super-indices indicating the system because we assume that the two systems are identical at all times. This system of equations has two fixed points or equilibrium solutions, which are the same as before and given by Eqs. (5.11) and (5.12). For $\hat{g} < 1$, there is a single fixed point, but for $\hat{g} > 1$ there are two steady state solutions. We can study the stability of the solutions by linearizing Eqs. (5.14)–(5.16):

$$\begin{pmatrix} B(t+1) \\ F(t+1) \end{pmatrix} = \begin{pmatrix} (P_n f + 2c) O_{jeq} - P_n f B_{eq} - c & 2c O^{(i)}_{jeq} - P_n f B_{jeq} - c \\ 1 & 1 - P_r \end{pmatrix} \begin{pmatrix} B(t) \\ F(t) \end{pmatrix}.$$

At the standard operation equilibrium, no failures fixed point, the linearization becomes

$$\begin{pmatrix} B(t+1) \\ F(t+1) \end{pmatrix} = \begin{pmatrix} P_n f + c & c \\ 1 & 1 - Pr \end{pmatrix} \begin{pmatrix} B(t) \\ F(t) \end{pmatrix} \tag{5.17}$$

and the eigenvalues are

$$\gamma_{1+} = \frac{1}{2}\left(1 - P_r + P_n f + c + \sqrt{(1 - P_r - P_n f - c)^2 + 4c}\right) \tag{5.18}$$

$$\gamma_{1-} = \frac{1}{2}\left(1 - P_r + P_n f + c - \sqrt{(1 - P_r - P_n f - c)^2 + 4c}\right). \tag{5.19}$$

For $\hat{g} = 1$ the largest eigenvalue γ_{1+} goes through 1. This indicates that the fixed-point solution Eq. (5.11) becomes unstable at this point.

Similar calculation evaluating the linearization at the second fixed point, Eq. (5.12), shows that this second fixed point is stable for $\hat{g} > 1$. The bifurcation is essentially a transcritical bifurcation and the stability is transferred from the fixed point Eq. (5.11) to the appearing second fixed point Eq. (5.12) as increases through $\hat{g} = 1$.

The left eigenvectors corresponding to the eigenvalues Eqs. (5.18) and (5.19) are

$$\vec{V}_{i+} = (\gamma_{i+} - 1 + P_r, c), \quad \vec{V}_{i-} = (\gamma_{i-} - 1 + P_r, c) \tag{5.20}$$

We can use these eigenvectors to calculate the eigenvalues from measured quantities, because by applying them on the left of Eq. (5.17), we obtain

$$\gamma_{i+} = \frac{(-1 + P_r + \gamma_{i+}, c) \cdot \begin{pmatrix} B(t+1) \\ F(t+1) \end{pmatrix}}{(-1 + P_r + \gamma_{i+}, c) \cdot \begin{pmatrix} B(t) \\ F(t) \end{pmatrix}} \tag{5.21}$$

$$\gamma_{i-} = \frac{(-1 + P_r + \gamma_{i-}, c) \cdot \begin{pmatrix} B(t+1) \\ F(t+1) \end{pmatrix}}{(-1 + P_r + \gamma_{i-}, c) \cdot \begin{pmatrix} B(t) \\ F(t) \end{pmatrix}} \tag{5.22}$$

From these expressions, we can derive a diagnostic to determine the eigenvalues from the numerical calculations. The expressions are

$$\begin{aligned}[\gamma_{i\pm}] = \frac{1}{2}\Bigg\{ & 1 - P_r + \frac{B(t+1)}{B(t)} - c\frac{F(t+1)}{B(t)} \\ & \pm \sqrt{\left[-1 + P_r + \frac{B(t+1)}{B(t)} - c\frac{F(t)}{B(t)}\right]^2 - 4\frac{(-1+P_r)F(t) + F(t+1)}{B(t)}c} \Bigg\}\end{aligned} \tag{5.23}$$

Here, we use the square brackets around the γ's to indicate that these values will be obtained from numerical results. They are diagnostics and should not be confused with the analytical value of the eigenvalues. Note that for $c = 0$, these two eigenvalues are

$$\left[\gamma_{1-}\right] = \frac{B\,(t+1)}{B\,(t)} \quad \text{and} \quad \left[\gamma_{1+}\right] = 1 - P_r. \tag{5.24}$$

The first one is identical to the standard metric used in determining criticality with respect to cascading events [11–13]. This metric is defined as

$$\lambda_B\,(t+1) = \frac{B\,(t+1)}{B\,(t)} \tag{5.25}$$

and measures the propagation of the failures. If λ_B is greater than 1, the number of failures increases with time and there is the possibility of a large cascading event. However, if λ_B is less than one, the failures will stop propagating and the failure size remains small. This measure has been introduced [17–19] on the basis of a branching process [20].

Having diagonalized the matrix in Eq. (5.17), one can solve the linear equations by iteration and one obtains

$$\begin{pmatrix} B\,(t+1) \\ F\,(t+1) \end{pmatrix} = \frac{B\,(1)}{\gamma_{i+} - \gamma_{i-}} \begin{pmatrix} \left[\gamma_{i+} - 1 + P_r\right]\gamma_{i+}^t - \left[\gamma_{i-} - 1 + P_r\right]\gamma_{i-}^t \\ \underbrace{\gamma_{i+}^t - \gamma_{i-}^t}_{O_{ieq}} \end{pmatrix}. \tag{5.26}$$

From this solution, we can calculate the propagation of the failures

$$\lambda_{iB}\,(t+1) = \frac{B\,(t+1)}{B\,(t)} = \frac{\left[\gamma_{i+} - 1 + P_r\right]\gamma_{i+}^t - \left[\gamma_{i-} - 1 + P_r\right]\gamma_{i-}^t}{\left[\gamma_{i+} - 1 + P_r\right]\gamma_{i+}^{t-1} - \left[\gamma_{i-} - 1 + P_r\right]\gamma_{i-}^{t-1}}. \tag{5.27}$$

However, this is the solution of the linear problem, it only make sense for $t \to \infty$ in the initial, linear, phase of the evolution. The asymptotic values for are meaningless. This ratio of failing components gives a measure of the propagation of the failures. Here we want to examine the relation between the cascading point, $\lambda_{\mathrm{ib}} = 1$, and the equilibrium bifurcation point, $\hat{g} = 1$, which for $\mathrm{c} = 0$ were the same. The important question is what is the proper diagnostic to measure the cascading threshold.

From Eq. (5.27) the first two values for the rate of propagation of failures are

$$\lambda_{1B}(2) = P_n f + c \tag{5.28}$$

$$\lambda_{1B}(3) = P_n f + c + \frac{c}{P_n f + c}. \tag{5.29}$$

As one can see in the case of coupled systems, Eq. (5.27) gives λ_{1B} as an increasing function of t. If the first value of λ_{1B} is greater than 1, the cascade will go on. This

is a sufficient condition for the cascade threshold. It is however not a necessary condition, because in a few initial steps the number of failures may first decrease till λ_{1B} becomes greater than one and increase again. How many steps can λ_{1B} be less than 1 without extinguishing the cascade is not clear, it will depend on the size of the initial perturbation. If we assume that three steps are sufficient, we can use Eq. (5.29) as a typical parameter controlling the cascade, then the cascading threshold is

$$P_n f = \frac{1}{2}\left(1 + \sqrt{1 - 4c}\right) - c. \tag{5.30}$$

Since c << 1 in the relevant cases, we can write this threshold in a more general way

$$P_n f = 1 - \mu c \tag{5.31}$$

where μ is a number of order 1 to be determined by numerical calculations.
Here, we see that the effect of the coupling is to reduce the cascading threshold by a factor of the order of c, while the equilibrium bifurcation point was reduced by a larger term of the order c/P_r.

5.5 Mean Field Theory: Numerical Solution

The mean field theory system of equations, Eqs. (5.14)–(5.16), can be solved numerically without any further assumptions. The nonlinear solutions of these equations will allow us to evaluate better the meaning of the analytical results described in the previous section and the validity of the linear approximations. Here, we consider systems with 10^4 components and the values of the couplings are $c = 0.0005$ and $P_r = 0.001$. For these parameters, the equilibrium bifurcation point, $\hat{g} = 1$, is at $P_{\mathrm{n}} f = 0.4995$.

In Fig. 5.8, we have plotted the fraction of failing components as a function of the iteration for different values of $P_{\mathrm{n}} f$. This plot gives a good description of the propagation of the failures. For all cases we have the used the same initial condition:

$$O_{init} = 1, B_{init} = \frac{1}{N}, \text{and} \quad F_{init} = 0 \tag{5.32}$$

where N is the total number of components. In this case, if B goes below 10^{-4} the cascade has effectively extinguished because the system has 10^4 components. However, for an initial condition with n failures, the cascade is extinguished for $B = n/N$.

In looking at the Fig. 5.9, it is clear that the cascading threshold is close to $P_{\mathrm{n}} f = 1$. We have repeated the calculation for $c = 0.05$ and $P_{\mathrm{r}} = 0.1$. These parameters are unrealistically large, and the steady state value of B is considerably larger than the initial value. In this case, below the cascading threshold the number of failures dips

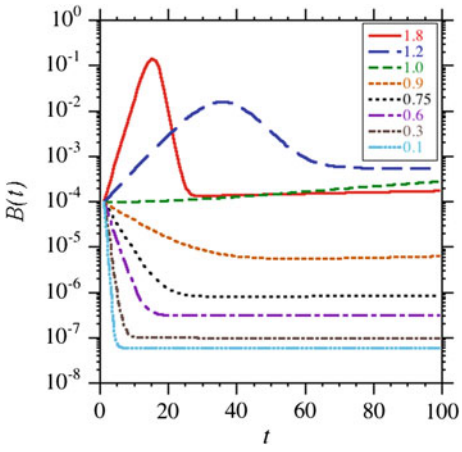

Fig. 5.8 The fraction of failing components as a function of the iteration for different values of $P_{\mathrm{n}} f$. In this case the parameters are $c = 0.0005$ and $P_r = 0.001$ and the critical value of $P_{\mathrm{n}} f$ is about 1

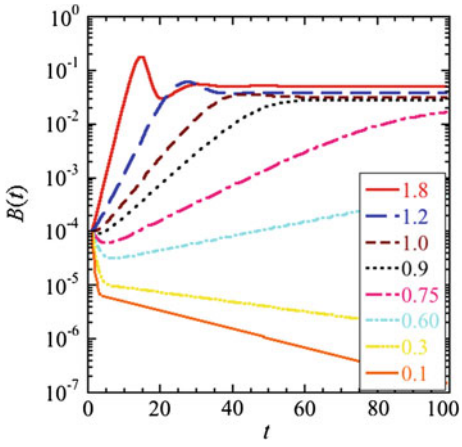

Fig. 5.9 The fraction of failing components as a function of the iteration for different values of $P_{\mathrm{n}} f$. In this case the parameters are $c = 0.05$ and $Pr = 0.1$ and the critical value of $P_n f$ is about 0.9

down well below 10^{-4} before rising again to the steady state value. The results are shown in Fig. 5.9. Because the equilibrium bifurcation point depends mostly on the ratio c/P_{r}, this change of parameters hardly changes the equilibrium bifurcation point. However, the cascading threshold depends on the value of c, therefore and as expected, the threshold for cascading is now close to $P_{\mathrm{n}} f = 0.9$.

From the previous analytical calculations and these numerical results we can draw two conclusions:

(1) The cascading threshold at which failures initially grow is not at the equilibrium bifurcation point. From the numerical calculations we can see that this threshold is consistent with Eq. (5.31). Therefore, the initial cascade propagation does not seem to be linked to the largest eigenvalue of the linear approximation to the mean field equations as it was for the decoupled systems.

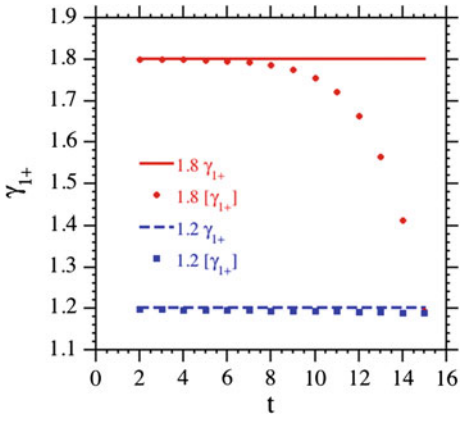

Fig. 5.10 The analytic and computed γ_{1+} eigenvalues for two values of $P_n f$

(2) In the cases above the cascading threshold, the cascade starting near the unstable fixed point (11) proceeds up to a certain size, and then decreases as the transient converges to the stable fixed point (12). This is a transient and nonlinear system effect, which is not taken into account in the linearization that is valid only near the fixed point (11).

The next step is comparing the calculated eigenvalues Eq. (5.23) with the analytical ones, Eqs. (5.16)–(5.19). We compare the measured eigenvalues from the numerical solution to the eigenvalues for the first fixed point because of the initial conditions taken here. For γ_{1+} and $P_n f < 1$, the analytical and numerical values are very close to 1 and any difference would be small. Therefore, we limit the numerical comparison to $P_n f > 1$.

In Fig. 5.10, we have plotted the γ_{1+} eigenvalue and the measured one, $[\gamma_{1+}]$ from the mean field numerical calculations for two values of $P_n f$. There the agreement is good. In Fig. 5.11, we have the same comparison for γ_{1-}. Again the agreement is very good. In particular, the agreement is expected to be better for the very low number of iterations, because no finite size effects are present. Note that γ_{1-} is the eigenvalue associated with the transition of the fixed point 1 to a fixed point 2.

The next step is to compare the propagation of failures from the linear calculation with the solution of the mean field theory. In Fig. 5.12, we compare λ_B, as calculated numerically from the nonlinear mean field theory in Eq. (5.25), with the value in Eq. (5.27) obtained from the linear approximation Eq. (5.26).

We see that the mean field theory gives a value for λ_B that increases with time. It is not constant as obtained from a branching process. Therefore this confirms the previous assumption that the cascade threshold can be calculated by Eq. (5.30).

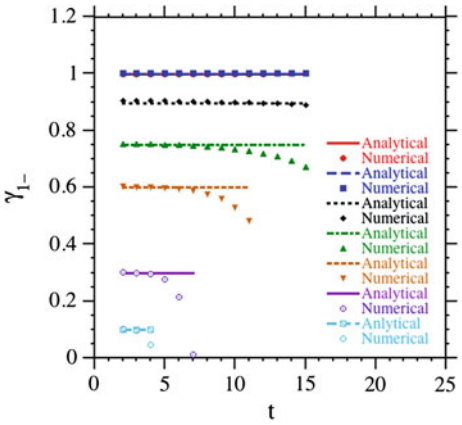

Fig. 5.11 The analytic and computed γ_{1-} eigenvalues for a number of values of $P_n f$

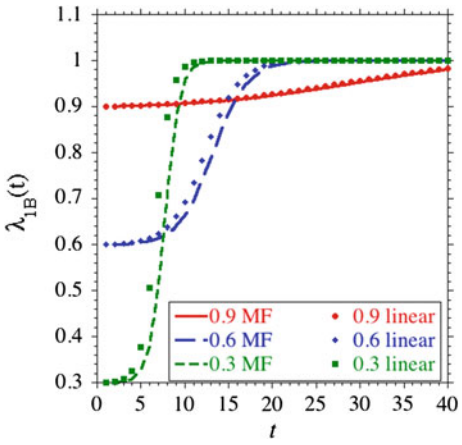

Fig. 5.12 Comparison of λ_B, as calculated numerically from the nonlinear mean field theory in Eq. (5.25), with the value in Eq. (5.27) obtained from the linear approximation

5.6 Application and Comparison to the Demon Model

Now that we have an understanding from the mean field theory of what should be measured, we can apply these measurements to the full dynamical model, Demon. In this case, the measurements will by necessity have a statistical character.

The equilibrium bifurcation is linked to the γ_{1-} eigenvalue. Therefore to get a sense of the equilibrium bifurcation point, we can apply the $[\gamma_{1-}]$ diagnostic, Eq. (5.23), to the Demon numerical calculations. The comparison between the analytical eigenvalue and the measured $[\gamma_{1-}]$ in Demon is shown in Fig. 5.13. The agreement is relatively good for a low number of iterations. As the number of iterations increases, finite size effects become important and the analytical and numerical results diverge, as we should expect. If instead of the linear analytical result we used the mean field theory result the agreement would be better.

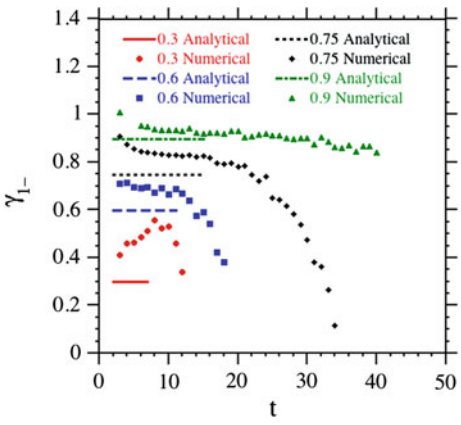

Fig. 5.13 The analytic and Demon γ_{1-} eigenvalues for a number of values of $P_n f$

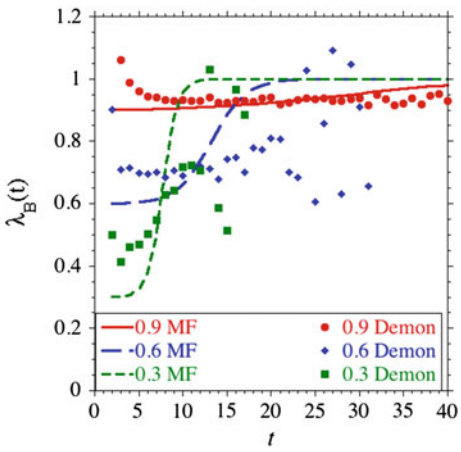

Fig. 5.14 Comparison between Demon and non-linear mean field (Eq. (5.30)) λ_B for a number of values of $P_n f$

The other relevant parameter is the rate of propagation of the cascades. We can compare λ_B in the Demon model with the one calculated from the mean field theory, Eq. (5.30). The result of this comparison is shown in Fig. 5.14. We can see that there is a basic agreement.

Both comparisons are poorer for low values of γ_{1-} and λ_B, because in this parameter region the data from Demon are scattered. The reason for that is that there is a very small number of cascading events and the statistical evaluation is poor.

5.7 Conclusions

The critical infrastructure systems upon which modern society relies often exhibit characteristics of complex dynamical systems operating near their critical point including heavy, power law, tails in the failure size distribution and long time cor-

relations. We as a matter of course take their smooth operation for granted and are typically shocked when one of these systems fails despite the fact that these failures are a completely inevitable result of the complex dynamical nature of the system. Though failures are inevitable, one can design and operate the systems to reduce the risk or at least be aware of what the risk is, making understanding these systems a high priority for ensuring security and social wellbeing. While modeling these individual systems themselves is a challenging and worthwhile exercise, in the real world they usually do not exist in a vacuum, instead being coupled, sometimes very tightly, to one or more other complex infrastructure systems. This coupling can lead to new behavior including modifications of the critical points and the weight of the tails. Realistically modeling these coupled infrastructure systems in a dynamic manner is a daunting task outside out current capabilities. For example, only recently has a simplified model of the electric power grid alone with cascading overloads and complex dynamics been validated with observed data [21]. Therefore simpler models that can capture some of the important characteristics have a significant role to play in understanding the risks associated with the structure and growth of these critical systems. Even the simple modeling of these coupled system leads to a very large parameter space that must be explored with different regions of parameter space having relevance to different coupled infrastructure systems. Within each of these parameter regimes there is a rich variety of dynamics to be characterized.

This chapter has attempted to look at a simple model, Demon, of coupled infrastructure systems that can both be simulated and attacked analytically using mean field theory. We have found that in the region of parameter space we have explored, the coupling between the systems reduces the critical point (the propagation parameter in this model which is related to the system loading in the real world) and makes the tail heavier. The reduction in the critical point is found both in the mean field theory and the Demon model. This reduction has serious implications for the real world as we load the systems more heavily and as the coupling becomes ever tighter, suggesting that the probability of large failures is likely to become more probable. The mean field theory does a better job of matching the numerical results when taken to higher order and is even able to capture the general time behavior of the propagation metric λ. This metric is one which can in principle be measured in the real world [22] as a state estimator. Using this it may be possible to give a statistical estimate of the risk of failure of various sizes, a needed function given the non-normal nature of these distribution functions. In addition, it has been found that the PDF of the failure sizes gains a heavier tail, with the slope going from ~ -1.0 to ~ -0.8. While this may not seem like a major change, because this is a power law it implies a significantly higher relative risk of the larger failures which are the failures that dominate the "cost" to society. These models find that even with weak interaction one cannot always safely ignore coupling.

Characterizing the dynamics in the different regimes is more than an academic exercise since as we engineer higher tolerances in individual systems and make the interdependencies between systems stronger we will be exploring these new parameter regimes the hard way, by trial and error. Unfortunately error in this case has the potential to lead to global system failure. By investigating these systems from

this high level, regimes to be avoided can be identified and mechanisms for avoiding them can be explored. These general relationships are then available to be verified either with more physically based models or with real data.

Acknowledgments We gratefully acknowledge support in part from NSF grants ECCS-0606003, ECCS-0605848, SES-0623985, SES-0624361 and CPS-1135825. Two of us (BAC and DEN) also grateful for a "Catedra de Excelencia" from Universidad Carlos III-Banco de Santander Project.

References

1. Richard G. Little, Toward More Robust Infrastructure: Observations on Improving the Resilience and Reliability of Critical Systems, in Proceedings of the 36th Annual Hawaii International Conference on System Sciences (HICSS'03).
2. S. M. Rinaldi, Modeling and Simulating Critical Infrastructures and Their Interdependencies, in Proceedings of the 37th Annual Hawaii International Conference on System Sciences (HICSS'04), (Big Island, HI, USA), IEEE Computer Society Press, Jan. 2004.
3. S. M. Rinaldi, J. P. Peerenboom, and T. K. Kelly, *Identifying, understanding, and analyzing critical infrastructure interdependencies*, IEEE Control Systems Magazine, p. 11, December 2001.
4. D. E. Newman, B. Nkei, B. A. Carreras, I. Dobson, V. E. Lynch, P. Gradney, Risk assessment in complex interacting infrastructure systems, *Thirty-eighth Hawaii International Conference on System Sciences*, Hawaii, January 2005.
5. B. A. Carreras, D. E. Newman, Paul Gradney, V. E. Lynch, and I. Dobson, Interdependent Risk in Interacting Infrastructure Systems, *40th Hawaii International Conference on System Sciences, Hawaii*, Hawaii, Jan 2007.
6. B. Drossel and F. Schwabl, Physica A 199, 183 (1993).
7. P. Bak, K. Chen and C. Tang, Phys. Lett. A 147, 297 (1990).
8. B.A. Carreras, V.E. Lynch, I. Dobson, D.E. Newman, Critical points and transitions in an electric power transmission model for cascading failure blackouts, Chaos, vol. 12, no. 4, December 2002, pp. 985–994.
9. I. Dobson, J. Chen, J.S. Thorp, B. A. Carreras, and D. E. Newman, *Examining criticality of blackouts in power system models with cascading events*, 35th Hawaii International Conference on System Sciences, Hawaii, Hawaii, Jan. 2002.
10. Charles Perrow, *Normal accidents*, Princeton University Press, 1984.
11. I. Dobson, B. A. Carreras, and D. E. Newman, A probabilistic loading-dependent model of cascading failure and possible implications for blackouts, *36th Hawaii International Conference on System Sciences, Maui*, Hawaii, Jan. 2003.
12. I. Dobson, B.A. Carreras, D.E. Newman, Probabilistic load-dependent cascading failure with limited component interactions, *IEEE International Symposium on Circuits and System, Vancouver*, Canada, May 2004.
13. I. Dobson, B. A. Carreras, and D. E. Newman, A loading-dependent model of probabilistic cascading failure, Probability in the Engineering and Informational Sciences 19 (1), 15–32.
14. D.E. Newman, B.A. Carreras, V.E. Lynch, I. Dobson, Exploring complex systems aspects of blackout risk and mitigation, Reliability, IEEE Transactions on 60 (1), 134–143
15. I. Dobson, B.A. Carreras, V.E. Lynch, D.E. Newman, Complex systems analysis of series of blackouts: Cascading failure, critical points, and self-organization, Chaos, vol. 17 no. 2, 26103
16. R. Gann J. Venable, E.J. Friedman, A.S. Landsberg, Behavior of coupled automata, Phys. Rev. E 69, 046116 (2004).
17. I. Dobson, B.A. Carreras, D.E. Newman, A branching process approximation to cascading load-dependent system failure. *37th Hawaii International Conference on System Sciences*, Hawaii, January 2004.

18. I Dobson, BA Carreras, DE Newman, Branching process models for the exponentially increasing portions of cascading failure blackouts, System Sciences, 2005, Proceedings of the 38th *Hawaii International Conference on System Sciences*.
19. I Dobson, KR Wierzbicki, BA Carreras, VE Lynch, DE Newman, An estimator of propagation of cascading failure, System Sciences, 2006. HICSS'06. Proceedings of the 39th *Hawaii International Conference on System Sciences*
20. T.E. Harris, Theory of branching processes, Dover NY 1989.
21. B.A. Carreras, D.E. Newman, I. Dobson, N.S. Degala, Validating OPA with WECC data, Forty-sixth Hawaii International Conference on System Sciences, Maui, Hawaii, January 2013.
22. I Dobson, Estimating the propagation and extent of cascading line outages from utility data with a branching process, IEEE Transactions on Power Systems 27 (4), 2116–2126